Journal of Hazardous Materials 176 (2010) 510–520

Contents lists available at ScienceDirect

Journal of Hazardous Materials

journal homepage: www.elsevier.com/locate/jhazmat

Adsorption mechanisms of removing heavy metals and dyes from aqueous solution using date pits solid adsorbent

Mohammad A. Al-Ghouti[a,*], Juiki Li[b], Yousef Salamh[b], Nasir Al-Laqtah[b], Gavin Walker[b], Mohammad N.M. Ahmad[b]

[a] Industrial Chemistry Centre, Royal Scientific Society, P.O. Box 1438, Amman, Jordan
[b] School of Chemistry and Chemical Engineering, Queen's University Belfast, Stranmillis Road, Belfast BT9 5AG, UK

ARTICLE INFO

Article history:
Received 27 October 2009
Received in revised form 8 November 2009
Accepted 9 November 2009
Available online 13 November 2009

Keywords:
Adsorption mechanisms
Metal ions (Cu^{2+} and Cd^{2+})
Methylene blue
Date pits
FTIR

ABSTRACT

A potential usefulness of raw date pits as an inexpensive solid adsorbent for methylene blue (MB), copper ion (Cu^{2+}), and cadmium ion (Cd^{2+}) has been demonstrated in this work. This work was conducted to provide fundamental information from the study of equilibrium adsorption isotherms and to investigate the adsorption mechanisms in the adsorption of MB, Cu^{2+}, and Cd^{2+} onto raw date pits. The fit of two models, namely Langmuir and Freundlich models, to experimental data obtained from the adsorption isotherms was checked. The adsorption capacities of the raw date pits towards MB and both Cu^{2+} and Cd^{2+} ions obtained from Langmuir and Freundlich models were found to be 277.8, 35.9, and 39.5 mg g^{-1}, respectively. Surface functional groups on the raw date pits surface substantially influence the adsorption characteristics of MB, Cu^{2+}, and Cd^{2+} onto the raw date pits. The Fourier transform infrared spectroscopy (FTIR) studies show clear differences in both absorbances and shapes of the bands and in their locations before and after solute adsorption. Two mechanisms were observed for MB adsorption, hydrogen bonding and electrostatic attraction, while other mechanisms were observed for Cu^{2+} and Cd^{2+}. For Cu^{2+}, binding two cellulose/lignin units together is the predominant mechanism. For Cd^{2+}, the predominant mechanism is by binding itself using two hydroxyl groups in the cellulose/lignin unit.

1. Introduction

The existence of heavy metals and dyes in the aquatic system can be detrimental to a variety of living species. Many industrial processes discharge aqueous effluents containing heavy metals and dyes. Heavy metals and dyes are non-biodegradable and tend to accumulate in living organisms, causing various diseases and disorders [1].

Over 7×10^5 tons of synthetic dyes are produced annually worldwide [2]. It is estimated that 10–15% of the dyes are lost in the dye effluent during such dyeing processes. The dyeing operations are of primary environmental concern for the textile industry for a number of reasons: dyeing is a water intensive process; large amounts of salt are often needed to improve dye fixation on the textile material; many dyes contain heavy metals (e.g. chromium and copper) as either a dye component or as a contaminant and unfixed dye releases high doses of color to mill effluent, as well as salt and metals [2].

Cadmium concentrations in the range 0.1–100 mg dm^{-3} are typical in wastewater from several industries (chemical and metal product facilities, leather and tanning processes, electricity and gas production and sanitary industries) [3]. Cadmium and copper, the metals considered in this study, are the widely used elements, where an intake of excessively large doses by man may lead to serious kidney failure and liver disease [4].

Accordingly, improved and innovative methods for water and wastewater treatment are continuously being developed to treat water-containing metals [1]. Various treatment techniques available for heavy metals and dyes are reduction, ion exchange, adsorption, reverse osmosis, and chemical precipitation [5]. Most of these methods suffer from drawbacks like high capital and operational costs and there are problems in disposal of the residual metal sludge [5]. The use of activated carbons to remove organic and inorganic pollutants from waters is widely extended, because of their high surface area, microporous characteristic, and the chemical nature of their surfaces. However, they are expensive and their regeneration cost is also high. So there is a dire need for low-cost and readily available materials for the removal of toxic pollutants from water [6].

A potential usefulness of raw date pits (RDP) as an inexpensive solid adsorbent for a number of metal ions has been demonstrated

* Corresponding author. Tel.: +962 65344701; fax: +962 65344806.
E-mail addresses: mghouti@rss.gov.jo, ghoutijo@yahoo.co.uk (M.A. Al-Ghouti).

0304-3894/$ – see front matter © 2009 Elsevier B.V. All rights reserved.
doi:10.1016/j.jhazmat.2009.11.059

earlier [7,8]. However, adsorption mechanisms of these metals onto the RDP were not fully investigated. Banat et al. [9] used raw date pits and date pit activated carbons for the adsorption of Zn^{2+} and Cu^{2+} ions from water. Activated date pit carbons were also used for the adsorption of cadmium ions and other organic compounds from water [10]. They studied the effect of contact time, pH, temperature, cadmium ion concentration, adsorbent dose, salinity, as well as the activation temperature on the removal of cadmium ions by date pits. Non-activated date pits exhibited higher Zn^{2+} and Cu^{2+} ion uptake than activated date pits. The uptake of both metal ions increased on increasing the pH value of the system from 3.5 to 5.0 as well as on decreasing the temperature from 50 to 25 °C. Adsorption capacities for the non-activated date pits towards Cu^{2+} and Zn^{2+} ions as high as 0.15 and 0.09 mmol g^{-1}, respectively, were observed.

Dates constitute part of a popular subsistence among the populace of the Middle Eastern peninsula [11]. The fruit of the date palm is composed of a fleshy pericarp and seed. Pits of date palm (seed) are a waste product of many date fruit processing plants producing pitted dates, date powders, date syrup, date juice, chocolate coated dates, and date confectionery [11]. At present, pits are used mainly for animal feeds in the cattle, sheep, camel, and poultry industries. However, value can be added in several food products [11]. Thus, potential applications include oil extraction from the pits or to use them as a dietary-fiber provider in bakery formulations. An additional function includes roasting RDP and making a caffeine-free drink which can substitute coffee when caffeine is a concern but a coffee-related flavor is desired [11].

Adsorption is undoubtedly the most important of the physicochemical processes responsible for the uptake of inorganic and organic substances in the aqueous environment. Factors such as pH, nature and concentration of substrate and adsorbing ion, ionic strength, and the presence of competing and complex ions affect the extent of adsorption. This work is also to explore the feasibility of using the RDP before and after chemical modification with microemulsions as adsorbents for the removal of heavy metals and dyes. The results of this study will be presented in the future publications.

Therefore, the present paper would report the salient features of the findings regarding the available functional groups, e.g. hydroxyl groups on the RDP and the adsorption profile of MB molecules, Cu^{2+}, and Cd^{2+} ions onto the RDP as an effective and low-cost solid extractor for the removal and/or concentration minimization of MB, Cu^{2+}, and Cd^{2+} ions species from aqueous and wastewater samples. This work was conducted to provide fundamental information from the study of equilibrium adsorption isotherms and to investigate the adsorption mechanisms for the adsorption of MB, Cu^{2+}, and Cd^{2+} from aqueous solution onto the RDP. The results summarized herein are also part of an investigation conducted to evaluate the adsorption capacities by taking into consideration the experimental parameters such as pH, particle size, and initial solute concentration. Moreover, the most probable adsorption mechanisms will also be fully investigated.

2. Experimental materials and methods

2.1. Chemicals

Deionized distilled water was used to prepare all solutions and suspensions. Stock solutions of metal ions were prepared from their sulfates ($CuSO_4{\cdot}4H_2O$, $CdSO_4$, analytical reagent grade, Fluka Chemie AG, Buchs, Switzerland). Methylene blue, Basic blue 9 ($C_{16}H_{18}N_3S^+Cl^-$, C.I. 52015, Fluka Chemie) was used. All solute standards were prepared by dissolving appropriate amount of solute into demonized water.

2.2. The adsorbent

The raw date pits were collected and washed with distilled water to be completely free from dirt and inherent pulp, dried at 105 °C for 3 h, and finally crushed to give a dark brown powder with different particle sizes (125–300, 300–500, and 500–710 μm). The approximate percentage of hemicellulose, lignin, and cellulose in typical date pits are 17.5, 11.0, and 42.5% dry weight, respectively [12].

2.3. Characterization of the raw date pits

The surface area of the adsorbent was obtained from nitrogen adsorption measurements made at liquid nitrogen temperature, 77 K and by using the Brunauer, Emmett and Teller (BET) equation. Solution pH and Fourier transform infrared (FTIR–PerkinElmer Spectrophotometer RXI) of the RDP were also studied. In addition, adsorbent samples were removed from the solute solution after equilibration and dried at 65 °C, to remove the water in preparation for the FTIR analysis. The spectra of the loaded-adsorbent were then recorded. A FTIR–PerkinElmer Spectrophotometer RXI was used in all investigations. Scanning electron microscopy (SEM, a JEOL-JSM 6400 apparatus) was also used for all samples.

2.4. Surface area and pore size analysis

The surface area of the RDP was obtained by using BET method and by assuming the section area of nitrogen molecule to be 0.162 nm^2 [2]. Nitrogen adsorption at 77 K is a standard and widely used method for determining surface area, pore volume and pore size distribution of the adsorbent. Nitrogen adsorption isotherms of the RDP were determined at 77 K using a nitrogen adsorption apparatus (quantachrome instruments NOVA e-series). The weight of the sample was around 0.4 g. The sample was outgassed under vacuum at 100 °C for 24 h before nitrogen adsorption. The aims of outgassing are: (i) to reach a well-defined intermediate state by the removal of physisorbed molecules and (ii) to avoid any drastic changes as a result of ageing or surface modification [13].

2.5. Equilibrium adsorption isotherms

The equilibrium isotherms are very important in designing adsorption systems. To estimate the adsorption characteristics of an adsorbent, the adsorption isotherm of that adsorbent with a specific adsorbate is registered. Concentration variation method is used to calculate the adsorption characteristic of adsorbent. It is mainly carried out by selecting an appropriate concentration range of the adsorbate with a fixed mass of adsorbent. The ratio of adsorbent mass and the volume of solute solution were 1:1 (g dm^{-3}).

Aqueous solutions of heavy metals (Cu^{2+} and Cd^{2+}) and methylene blue (MB) were prepared in a final concentration of 1–50 and 50–900 mg dm^{-3} with 5 and 50 mg dm^{-3} intervals, respectively. The adsorption isotherm experiments were carried out in 100 cm^3 glass bottles where 0.05 g of the RDP and 50 cm^3 of the appropriate concentration of the test solute solution were added. The bottle samples were subsequently capped and shaken in a shaker (Gerhardt Bonn type 655) for 72 h at 20 °C (room temperature) and 80 rpm. The particle size range from 125 to 710 μm was used. The pH of the solutions was adjusted to its appropriate value by adding either 1 M HCl or 1 M NaOH (pH range from 2 to 10). After 72 h, equilibrium was reached and equilibrium concentration was estimated. The samples were filtered through a 0.45 μm cellulose nitrate membrane filter (Swinnex-25 Millipore). Duplicate samples were measured and the standard error in the readings was less than 3%. Blanks were also used.

The initial and equilibrium Cu^{2+} and Cd^{2+} concentrations were determined using inductively coupled plasma (ICP) (an IRIS Intrepid by ThermoFisher Scientific). The initial and equilibrium MB concentrations were determined using a PerkinElmer UV–Vis spectrophotometer corresponding to λ_{max} of MB dye. The concentrations were calculated using the Beer–Lambert equation [2]:

$$\text{Absorbance} = \varepsilon C_s l \quad (1)$$

where ε is the molar absorptivity, C_s the concentration of sample, and l the thickness of the absorbing medium (1 cm).

Percentage of solute removal was then calculated as follows [2]:

$$\text{Removal}\,(\%) = \frac{C_i - C_e}{C_i} \times 100\% \quad (2)$$

where C_i and C_e are the initial and equilibrium solute concentrations (mg dm^{-3}), respectively.

2.6. Desorption studies

Desorption study was performed using H_2O, HCl (1 mol dm^{-3}), and NaOH (1 mol dm^{-3}) as eluent solutions. These experiments were performed by immersing the RDP in 50 cm^3 of eluent solution for 72 h with stirring at 80 rpm. The bulk solute concentration in solution was measured as previously described. The extent of desorption was calculated from Eq. (3) [2].

$$\text{Desorption}\,(\%) = \frac{\text{desorbed amount of solute}}{\text{absorbed amount of solute}} \times 100 \quad (3)$$

2.7. FTIR spectroscopy

FTIR spectra were recorded between 4000 and 400 cm^{-1}. Discs were prepared by first mixing 1 mg of dried sample with 500 mg of KBr (Merck, for spectroscopy) in an agate mortar and then pressing the resulting mixture successively at 8 tons cm^{-2}.

3. Results and discussion

3.1. Effect of pH value

Preliminary investigations showed that the equilibrium is attained in 72 h. In these experiments, the initial pH of solute containing solution was adjusted to the desired value (pH value: 2–11) using either 1 M HCl or 1 M NaOH solution. To the pH adjusted solute solution, the RDP was added. The effect of pH on the percentage of solute removal from aqueous solution by the RDP is illustrated in Fig. 1. The figure shows the maximum percentage removal of the MB from aqueous solution taking place at pH (pH 4–10), and that the removal percentage decreases with the decrease in pH. Lower adsorption of MB at low pH is probably due to the presence of excess H^+ ions competing with the cation groups on the dye for the adsorption sites [2]. The percentage removal of the Cd^{2+} decreased with further increase in pH (above pH 10), and the slightly constant removal rate was achieved under acidic and basic conditions (pH 2–10). Variation in pH can affect the surface charge of the adsorbent and the degree of ionization and speciation of the metal adsorbate [14]. As the surface charge density decreases with an increase in the solution pH, the electrostatic repulsion between positively charged dye (MB) and the surface of the RDP is lowered, which may result in an increase in the rate of adsorption [15]. An optimum pH range usually between pH 4.0 and pH 6.0 leaves the binding sites unprotonated and metal binding is maximized. At pH values above this optimum range, most metals tend to precipitate out of solution in the hydroxide form [14].

Metal ion uptake in the RDP may involve complexation, coordination, chelation, ion exchange, and adsorption [16]. In addition, electrostatic attraction and hydrogen bonding may be involved in the adsorption behavior of MB in the RDP [2]. This pH dependence of the binding showed that ion exchange, electrostatic interactions, and other phenomena are involved in the binding mechanism of metal cations by the RDP [16]. Indeed, adsorption and/or chelation involving hydroxyl functions may increase the binding level of Cu^{2+} and Cd^{2+} ions in addition to the electrostatic interactions taking place [17]. In the ion-exchange mechanism, metal ions bind

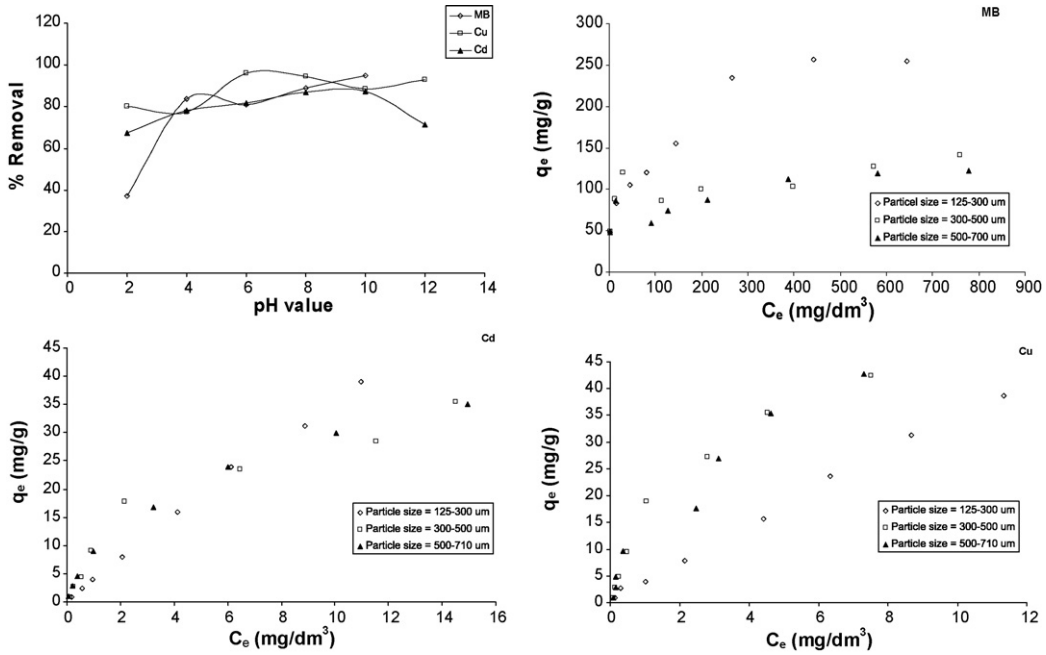

Fig. 1. The effect of pH and particle sizes of adsorption of MB, Cu^{2+}, and Cd^{2+} onto the RDP. Experimental conditions: mass of the RDP = 0.05 g, volume of solution = 50 cm^3, equilibrium time = 72 h, temperature = 20 °C and shaking speed = 80 rpm and pH of solute solution (effect of particle sizes) = 4.0. For pH dependency: particle size 125–300 μm, temperature = 22 °C, initial MB concentration = 100 mg dm^{-3}, and initial Cu^{2+} and Cd^{2+} concentration = 50 mg dm^{-3}.

to anionic sites by displacing protons from acidic groups [16]. In the complexation mechanism, metal ions sequestration is viewed as the coordination of metal ions to surface functional groups [16]. It was confirmed that the RDP is dominated by negatively charged sites that are largely hydroxyl groups. The extent of Cu^{2+} and Cd^{2+} adsorption from aqueous solutions is strongly influenced by the chemistry and surface morphology of the RDP, for example; the interaction of metal ions on surface cellulose hydroxyl groups (cellulose-OH); hydrogen bonding of hydrated metal ions with glucose from mostly cellulose and formation of complexes with surface [16].

The RDP is acidic in nature ($pH_{solution}$ 4.6) due to the presence of various functional groups that include alcohols, phenolic hydroxides, and ethers. Cu^{2+} and Cd^{2+} ions may form complexes with surface functional groups of the RDP such as cellulose-OH and phenolic-OH through ion-exchange reactions (see Section 3.4.). At lower pH (that is under acidic condition), the functionality of these groups is not changed. At higher pH, these groups begin to neutralize changing their activity and binding properties. The probable binding mechanism for various functional groups will be discussed in Section 3.4. A slightly constant behavior for Cu^{2+} and Cd^{2+} was observed between pH values 2 and 10.

3.2. Effect of particle sizes

Understanding the mechanisms of heavy metals and dyes adsorption on the RDP surface is essential for an effective removal of these solutes from wastewaters. The breaking down of the large particle to form smaller ones probably serves to open the sealed channels in the adsorbent, which then becomes available for adsorption. As shown in Fig. 1, the size of the particle investigated in this work has little effect on solute adsorption onto the RDP at low initial solute concentrations as expressed by the total surface area when the particle size changed from (125–300) to (500–710) μm. However, this effect was noted for MB, Cu^{2+}, and Cd^{2+} at equilibrium concentrations higher than 100, 2, and 2 mg dm^{-3}, respectively. This behavior indicates that the mechanisms of adsorption did not depend on the particle size alone (i.e. surface area or channels) [2].

Fig. 1 shows that the amount of solute adsorbed increases with the decrease in particle size of the adsorbent. This is mainly true since the surface area and the number of active pores of the adsorbent increase with the decrease in particle size. Solute adsorption onto the adsorbent is also dependent on pore size distribution and will depend on the number of micro-, meso-, and macropores in the structure [18]. Solutes (MB, Cu^{2+}, and Cd^{2+}) which have different molecular structures (size, branching, and polarity), will be adsorbed to varying extent depending on the availability of pores of appropriate size [18].

The adsorption isotherms data were further analyzed using the Langmuir and Freundlich's models, which are the most frequently applied models [19]. The experimental data were fitted to by the Langmuir (Eq. (4)) and Freundlich equations (Eq. (5)), respectively, to describe the solutes adsorption [19,2]. The Eq. (4) is given by

$$q_e = \frac{X}{m} = \frac{K_L C_e}{1 + a_L C_e} \quad (4)$$

where q_e is the equilibrium solid phase solute concentration. It is usually expressed as the amount of solute adsorbed per unit mass of adsorbent (mg g^{-1}), X the amount of solute adsorbed (mg), m the mass of adsorbent (g), K_L the adsorption constant (dm^3 g^{-1}), C_e the equilibrium liquid phase concentration (mg dm^{-3}), a_L the Langmuir isotherm constant (dm^3 g^{-1}); it is related to K_L by $Q_{mon} \cdot a_L = K_L$ and Q_{mon} is the Langmuir monolayer capacity. The Eq. (5) has the form

$$q_e = K_F C_e^{1/n} \quad (5)$$

where K_F is the Freundlich isotherm constant (mg g^{-1} (mg dm^{-3})^n) which is an indicator of the adsorption capacity and n refers to adsorption tendency. Linear plot of log q_e vs. log C_e is obtained from the model and K_F and $1/n$ can be determined from the slope and intercept. The value of $1/n$ is indicative of the relative energy distribution on the adsorbent surface.

The fit of two models to the experimental data obtained from the adsorption isotherms was checked and the results are shown in Table 1. For Langmuir model, C_{eq}/q_e vs. C_e plot was constructed from the experimental data of MB. These are non-linear plots. In other words, it indicates that there was a heterogeneous adsorption. Moreover, the experimental data were well fitted with the Freundlich model. The Langmuir isotherm was not used to evaluate the experimental results of Cu^{2+} and Cd^{2+} since the experimental adsorption isotherms data (C_e vs. q_e) were slightly linear and did not fit with typical Langmuir isotherm form. However, the linear isotherm is appropriate for adsorption relationships in which the energetics of adsorption is uniform with increasing concentration and the loading of the adsorbent is low [20].

When the data of MB adsorption onto the RDP were plotted according to Langmuir linearized isotherm, two lines were obtained at low and high concentrations. This indicates the existence of two different types of adsorption sites with a wide spectrum of binding energies on the surface of the adsorbent [21]. The surface sites with highest energy are occupied first [22]. This behavior could be explained as follows: (i) the Coulomb attraction between

Table 1
Langmuir and Freundlich equation parameters for adsorption of MB, Cu^{2+}, and Cd^{2+} onto the RDP at various particle sizes.

Particle size (μm)	Langmuir parameters—MB (the whole concentration range)			Freundlich parameters—MB	
	K_L (dm^3 g^{-1})	a_L (dm^3 mg^{-1})	Q_{mon} (mg g^{-1})	K_F (mg g^{-1})(mg dm^{-3})^n	$1/n$
125–300	4.496	0.016	281	93.5	0.299
300–500	3.759	0.027	139	278.1	0.124
500–710	2.226	0.017	131	148.3	0.138

	K_F (mg g^{-1})(mg dm^{-3})^n	$1/n$	Equation	Adsorption capacity (mg g^{-1})*
Freundlich parameters—Cu^{2+}				
125–300	0.027	0.815	$\log q_e = 0.6959 + 0.815 \log C_e$	35.90
300–500	1.975	0.807	$\log q_e = 1.0704 + 0.807 \log C_e$	59.89
500–710	1.621	0.735	$\log q_e = 1.0495 + 0.735 \log C_e$	48.39
Freundlich parameters—Cd^{2+}				
125–300	0.0074	0.946	$\log q_e = 0.6126 + 0.946 \log C_e$	39.57
300–500	0.1327	0.705	$\log q_e = 0.8171 + 0.705 \log C_e$	43.26
500–710	0.2738	0.624	$\log q_e = 0.8785 + 0.624 \log C_e$	40.88

* Adsorption capacities correspond to the final equilibrium concentration at C_o = 50 mg dm^{-3}. Experimental conditions: mass of the RDP = 0.05 g, volume of solution = 50 cm^3, equilibrium time = 72 h, temperature = 20 °C and shaking speed = 80 rpm and pH of solute solution = 4.0.

the adsorbent and the adsorbate decreases as the MB molecules adsorb, because the surface charge becomes more positive, (ii) there are unfavorable chemical interactions between adjacent adsorbed species and (iii) variety of active sites on the adsorbent; as a result a variety for the adsorbate [23]. Allen et al. [22] explained the deviation from linearity as follows: when all of the available monolayer sites are taken up then some fresh internal surface can be created. The creation of the additional surface arises from the pressure of adsorbate molecules forcing into the macropore and micropore structures. Moreover, the adsorbate molecules can be linked to molecular wedges creating access to new surfaces and effectively clearing blocked pores [22]. Thus, this process tends to further increase the adsorptive capacities of the adsorbent.

The behavior of adsorption processes of Cu^{2+} and Cd^{2+} onto the RDP is almost linear and consequently, the Langmuir adsorption isotherm was not successfully applied. Langmuir isotherm was not utilized to evaluate the results, since the obtained adsorption isotherms did not present the typical Langmuirian form. The experimental evidence indicates that an isotherm plateau was not reached. The adsorption isotherms exhibited the Freundlich behavior, which indicates a heterogeneous surface binding [21]. The Freundlich adsorption equation predicts that the solute concentrations on the adsorbent will increase so long as there is an increase in the solute concentration in the aqueous solution. The values of q_e were predicted by introducing corresponding values of K_F and $1/n$ as well as the final Cu^{2+} and Cd^{2+} concentrations (C_o = 50 mg dm^{-3}) and the results are shown in Table 1. Therefore, it is clear from the experimental results that the adsorption capacities corresponding to the final equilibrium concentration were increased in order: $Cu^{2+} > Cd^{2+}$ at particle sizes higher than 125–300 μm. This behavior could be explained by the capability of Cu^{2+} ions to form a stable complex with the RDP would be higher at big particle sizes. The $1/n$ value from the Freundlich equation indicates that the relative distribution of energy sites depends on the nature and strength of the adsorption process. For example, the value of $1/n$ of adsorption Cu^{2+} onto the RDP surface is 0.815, in fact this value refers to 82% of the active sites that have equal energy where adsorption took place. Moreover, the values of n closer to 1 indicates homogeneous surface.

3.3. Surface area and pore size analyses

Nitrogen adsorption–desorption isotherms were recorded for the RDP and are shown in Fig. 2. A hysteresis loop was observed in the relative pressure range 0.05–1.0. The uncommon Type III isotherm, which is usually associated with water vapor adsorption, was observed for the RDP as well as low-pressure hysteresis. The adsorbent–adsorbate interactions, in this type, are weak as compared with the adsorbate–adsorbate interactions [24]. The shoulder of the hysteresis loop of desorption branch runs parallel to the adsorption curve. This could be explained in terms of the swelling of the particles, which accompanies adsorption. The swelling distorts the structure, for example by prising apart weak junctions between primary particles and opens up cavities which were previously inaccessible to adsorbate molecules. Since the distortion is not perfectly elastic, some molecules become trapped and can escape only very slowly, or possibly not at all, during the desorption run [25].

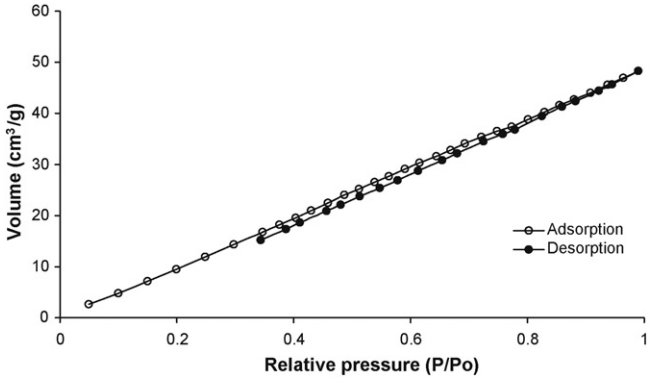

Fig. 2. Nitrogen adsorption isotherms at 77 K of the RDP. Experimental conditions: outgas temperature: 100 °C, outgas time: 1.0 h, sample weight: 0.0390 g, bath temperature: 273.0 K, analysis time: 722.1 min, adsorbate: nitrogen, and molecular weight: 28.013 g mol^{-1}.

To estimate the surface area of the adsorbent, the BET equation was applied to P/Po ranges of the N_2 isotherms [26–28]:

$$\frac{P}{V_n(Po - P)} = \frac{1}{V_m c} + \frac{c-1}{V_m c}\frac{P}{Po} \quad (6)$$

Here V_n is the volume of nitrogen adsorbed at pressure P, Po is the standard vapor pressure of the liquid at the temperature of experiment, V_m is the volume equivalent to an adsorbed monolayer, and c is the BET constant which is related to molar energy of adsorption in the first monolayer.

For the BET equation, the range of linearity is usually restricted to the P/Po values between 0.05 and 0.35. A plot of $P/V_n(Po - P)$ vs. P/Po over the approximate range $0.05 \leq P/Po \leq 0.35$ yields a straight line from which the monolayer capacity V_m can be evaluated. From the obtained V_m value, the specific surface area S_{BET} can be calculated by using the cross-sectional area of nitrogen of 0.162 nm. The surface area was calculated from the slope and y-intercept of the linear region of the BET transformation vs. relative pressure plot. The specific surface area, S_{BET}, is then calculated from V_m by [26]

$$S_{BET} = \frac{V_m n_a a_m}{m V_L} \quad (7)$$

where n_a is Avogadro number (6.022×10^{23} molecule mol^{-1}), a_m is the cross-section area occupied by each nitrogen molecule (0.162 nm^2), m is weight of the sample, and V_L is the molar volume of nitrogen gas (22.414 dm^3 mol^{-1}) [26].

The results of surface area and monolayer capacity of the adsorbent estimated from BET method are 80.49 m^2 g^{-1} and 0.023 cm^3 g^{-1}, respectively. The c value of the BET equation is related to the enthalpy of adsorption in the first adsorbed layer, i.e. an indication of the magnitude of the adsorbent–adsorbate interaction energy [27]. A high value of the parameter c is an indication of strong adsorbent–adsorbate interaction.

The lower c value (c = 2.8) obtained for the RDP may be related to its macroporosity and mesoporosity. The adsorption capacity of the RDP is expected to be weak which is anticipated from the lower N_2 monolayer adsorption capacity values, V_m.

Once the values of monolayer adsorption capacities are calculated from the BET equation, the BET surface area was estimated by multiplying the value of V_m by the molecular surface area of N_2 (0.162 nm^2 or 16.2×10^{-20} m^2) [28]. The BET plots are linear for the P/Po region taken for calculation of the surface area and V_m. The average pore radius and total pore volume of the RDP are 18.042 Å and 0.0726 cm^3 g^{-1}, respectively.

3.4. Desorption experiments

The experimental results showed less Cu^{2+} desorption in the neutral (0.04%) and acidic (0.05%) solutions after an equilibration time of 72 h. This was a reasonable result because under those conditions, the Cu^{2+} adsorption affinity on the RDP is high (Fig. 5) making the surface metal complexes stable. On the contrary, slightly larger amounts of Cd^{2+} and MB were desorbed in neutral and acidic solutions. The desorption percentage of Cd^{2+} in

neutral and acidic solutions is 0.10 and 0.67%, respectively, while the desorption percentage of MB in neutral and acidic solutions is 0.62 and 0.34%, respectively.

Cd^{2+} ions were desorbed generally to a higher extent in relation to Cu^{2+} under the same experimental conditions. This indicates that Cu^{2+} has higher adsorption affinity on the RDP than Cd^{2+}. This behavior will be discussed in details in Section 3.5.

3.5. Proposed mechanisms of adsorption

Understanding the mechanisms of the solute adsorption onto the RDP surfaces is essential for the removal of these from aqueous solution. The driving force for adsorption results from: (i) specific character of the solute relative to the particular solvent (i.e. solubility) and (ii) specific affinity of the solute for the solid. This kind of attraction may be predominantly one of electrical, van der Waals, or of a chemical nature. Consequently, the surface chemistry of the adsorbent and its effect on the adsorption process were investigated in order to interpret the solute adsorption.

FTIR spectroscopy is a useful tool for studying the interaction between an adsorbate and the active groups on the surface of the adsorbent. Parameters like pH and particle size play very important roles in determining the adsorption mechanisms. This work extensively illustrates the mechanisms of the MB, Cu^{2+}, and Cd^{2+} adsorption by taking into account the effect of these parameters on the adsorption process. A systematic approach relating the MB, Cu^{2+}, and Cd^{2+} adsorption performance of the RDP to its surface chemistry was tackled.

In this adsorption behavior, the interpretation of the FTIR is based on the chemical structure of the RDP. The RDP consists of three main components, namely cellulose, hemicellulose, and lignin, besides other minor constituents such as oil, protein, etc. [29]. Cellulose is a linear polymer with β-D-glucopyranose units and insoluble in water, hemicellulose is a low molecular weight chemically ill-defined polysaccharide, so it can be dissolved in water [29]. Both cellulose and hemicellulose contain majority of oxygen functional groups which are present in the lignocellulosic material such as hydroxyl, ether, and carbonyl, as shown in Fig. 3, while lignin is a complex, systematically polymerized, highly aromatic substance, and acts as a cementing matrix that holds between and within both cellulose and hemicellulose units [29].

The presence of these groups on the RDP surface substantially influences the adsorption characteristics of MB, Cu^{2+}, and Cd^{2+} onto the RDP. However, the adsorption tendency of the adsorbent may not be explained only based on physical properties such as surface area and pore diameter. Consequently, it is proposed that the mechanisms of adsorption may relate to the dispersion forces, complexation, hydrogen bond, or electrostatic interaction [2].

The adsorption mechanisms of MB, Cu^{2+}, and Cd^{2+} on the RDP were investigated and the results are shown in Fig. 4. For the RDP, a strong inter/intra-hydrogen bonded (O–H) stretching absorption is seen at 3400 cm^{-1}. Both intra- and intermolecular hydrogen bonding occur in cellulose. The detailed structure of this hydrogen bond network is shown in Fig. 4. In addition, there are many well-defined peaks in the fingerprint region between 1800 and 600 cm^{-1}: 1744 cm^{-1} for unconjugated C=O in xylans (hemicellulose), 1449 cm^{-1} for C–H deformation in lignin and carbohydrates, 1375 cm^{-1} for C–H deformation in cellulose and hemicellulose, 1320 cm^{-1} for C–H vibration in cellulose, 1246 cm^{-1} for syringyl ring and C–O stretch in lignin and xylan, 1156 cm^{-1} for C–O–C vibration in cellulose and hemicellulose, 1058 cm^{-1} for C–O stretch in cellulose and hemicellulose and 869 cm^{-1} for C–H deformation in cellulose [30].

Fig. 5 shows the FTIR spectra of the four samples in the fingerprint region between 1800 and 850 cm^{-1}, corresponding to the RDP, RDP-MB loaded, RDP-Cu^{2+} loaded, and RDP-Cd^{2+} loaded. Clear differences can be detected in the infrared spectra, both in the different absorbances and shapes of the bands and in their locations.

The 3000–2800 cm^{-1} region of the C–H stretch in the methyl and methylene groups was present in different proportions. These bands, which were mainly attributed to methoxyl groups, were higher for Cu^{2+} and Cd^{2+} and show relatively lower absorbance for MB.

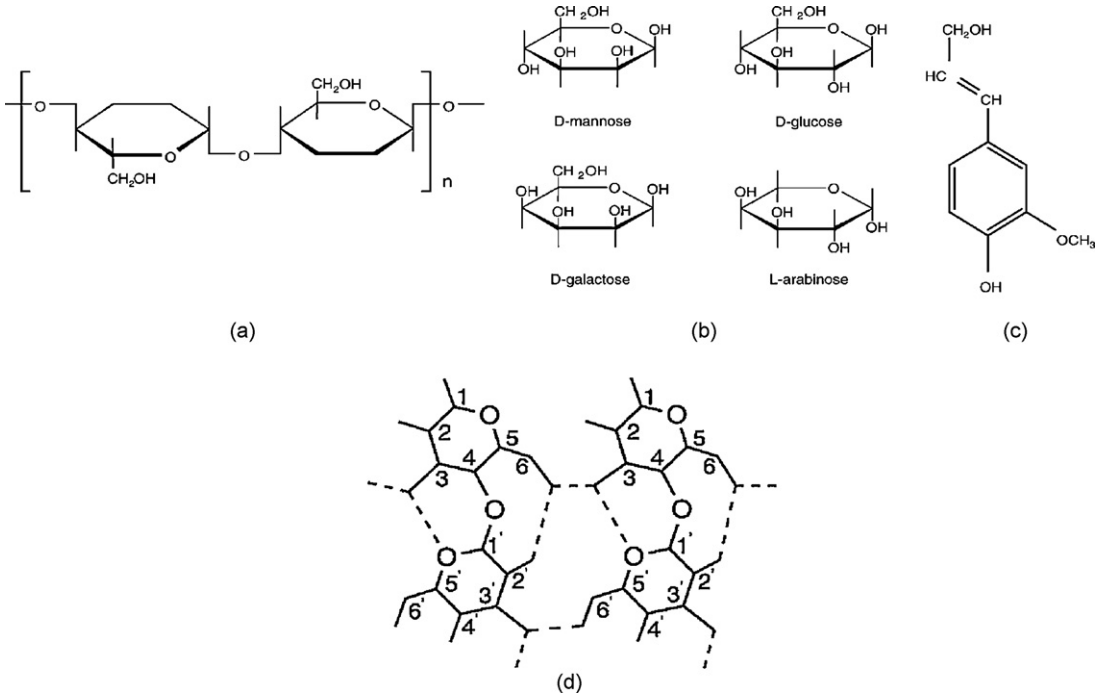

Fig. 3. (a) Cellulose molecule, (b) principal sugar residues of hemicellulose, (c) phenylpropanoid units found in lignin (El-Hendawy [29]) and (d) hydrogen bond system of cellulose samples.

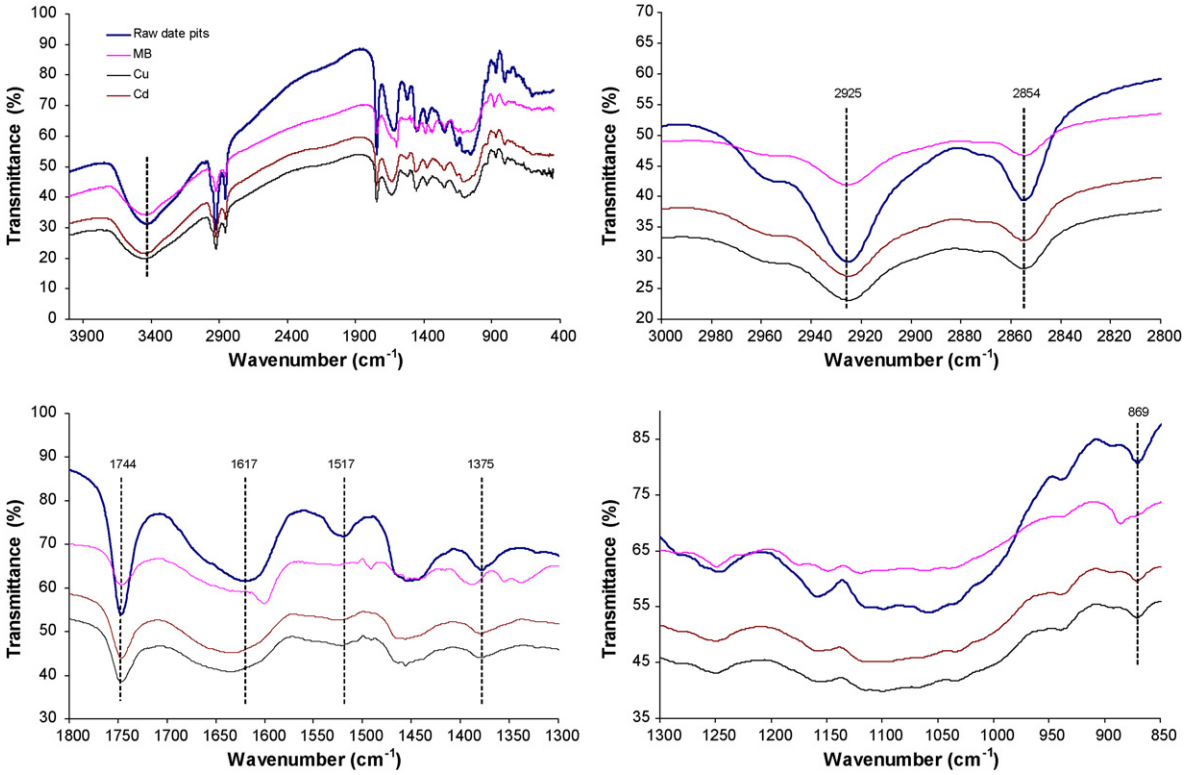

Fig. 4. FTIR spectra of the RDP, RDP-MB loaded, RDP-Cu^{2+} loaded, and RDP-Cd^{2+} loaded.

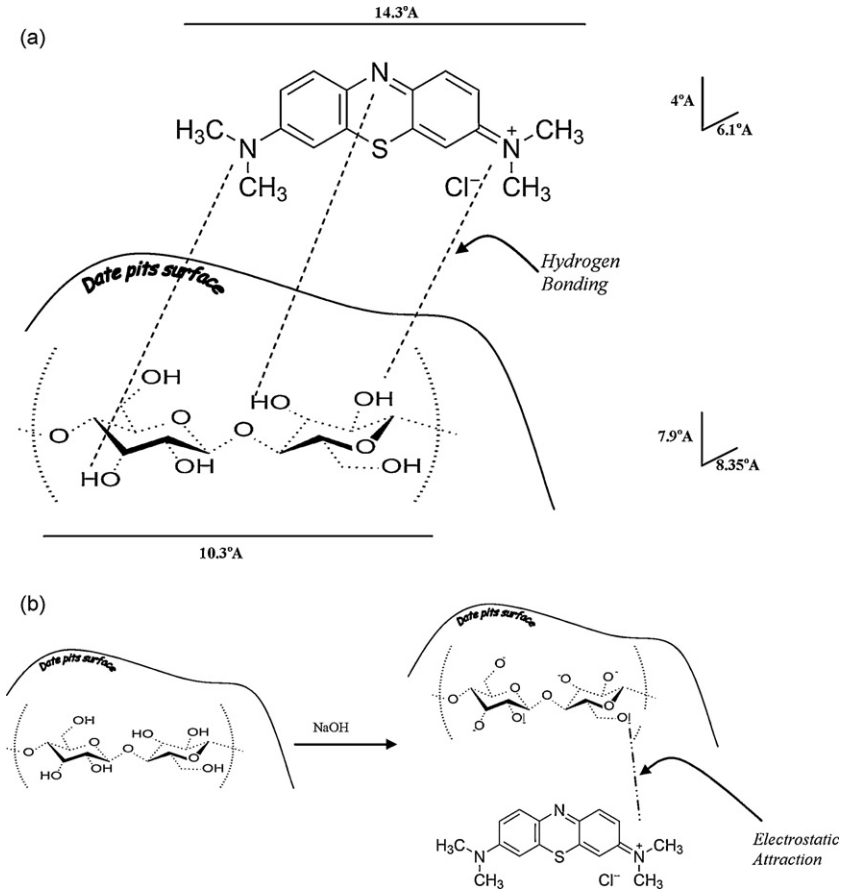

Fig. 5. Schematic representation of (a) hydrogen bonding between nitrogen atoms of MB and hydroxyl groups on the RDP surface, cellulose unit, and (b) electrostatic attraction between MB and the RDP surfaces, cellulose unit.

Between 1300 and 1000 cm^{-1}, the bands and peak ratios were very different due to various vibrations modes such as C–O, C–H, and C=O.

Upon analysis of the FTIR spectra, we see that the intensity decrease of the band at 1740 cm^{-1} is slightly higher in Cu^{2+} and Cd^{2+} than in MB. This is probably due to the different mechanisms of adsorption. Another significant difference is found in the MB spectrum where a doublet can be detected at 1610–1595 cm^{-1}, assigned to lignin, while only one band at 1610 cm^{-1} can be found in the Cu^{2+} and Cd^{2+} spectra. Thus, it seems that this type of functional group is likely to participate in metal binding. The doublet of this band is attributable to the difference in the mechanisms of adsorption.

In the spectral region assigned to cellulose C–O–C bridges, the infrared bands are slightly shifted in the case of MB. The band is located at 1158 cm^{-1} for the RDP, RDP-Cu^{2+} loaded, and RDP-Cd^{2+} loaded, and is shifted to 1149 cm^{-1} for MB. However, he intensity, for both RDP-Cu^{2+} loaded and RDP-Cd^{2+} loaded bands is reduced.

3.5.1. Proposed mechanisms of methylene blue adsorption

Shifts or changes of FTIR peaks indicate interactions of the solute with functional groups on the surface. It was shown that MB was adequately adsorbed for pH between 2 and 11, which may be due to the formation of surface hydrogen bonds between the hydroxyl groups on the RDP surface and the nitrogen atoms of MB as suggested in Fig. 5. Kaewprasit et al. [31] studied the adsorption of MB on cotton fiber (cellulose structure). It was assumed that a complete adsorption of MB as a monolayer onto the surface of the cotton fibers by forming a hydrogen bond between the surface of the cotton fiber and the nitrogen and sulfur of MB molecules was formed. Juang et al. [32] studied the mechanisms of adsorption of phenol and 3-chlorophenol from water using activated carbon prepared from plum kernels. The large number and array of different functional groups on the activated carbon surface (e.g. carboxylic, hydroxyl, carbonyl, etc.) implied existence of many types of adsorbent–solute interaction. It was suggested that because phenol and 3-chlorophenol have a pK_a of 9.92 and 9.43, respectively, they exist primarily in undissociated form in water before and after adsorption (pH < 8.19). The reaction-controlling mechanism may be partly due to hydrogen binding between the hydroxyl groups of phenols and the functional groups such as carboxylic on the activated carbon surface.

Moreover, in the desorption studies, the adsorption of MB onto the RDP resulted in formation of a stable chemical bond between the RDP surface and the MB molecules, which prevented the dye molecules from being eluted from the RDP surface. However, small amount of MB molecules were eluted (~0.6%), suggesting that a weak hydrogen bond was formed between MB molecules and surface of the RDP. Nevertheless, a large amount of the adsorbed dye was bound by formation of strong chemical bonds of ionic types [33]. Fig. 5 illustrates the electrostatic attraction between MB molecules and the cellulose-O^- on the RDP surface.

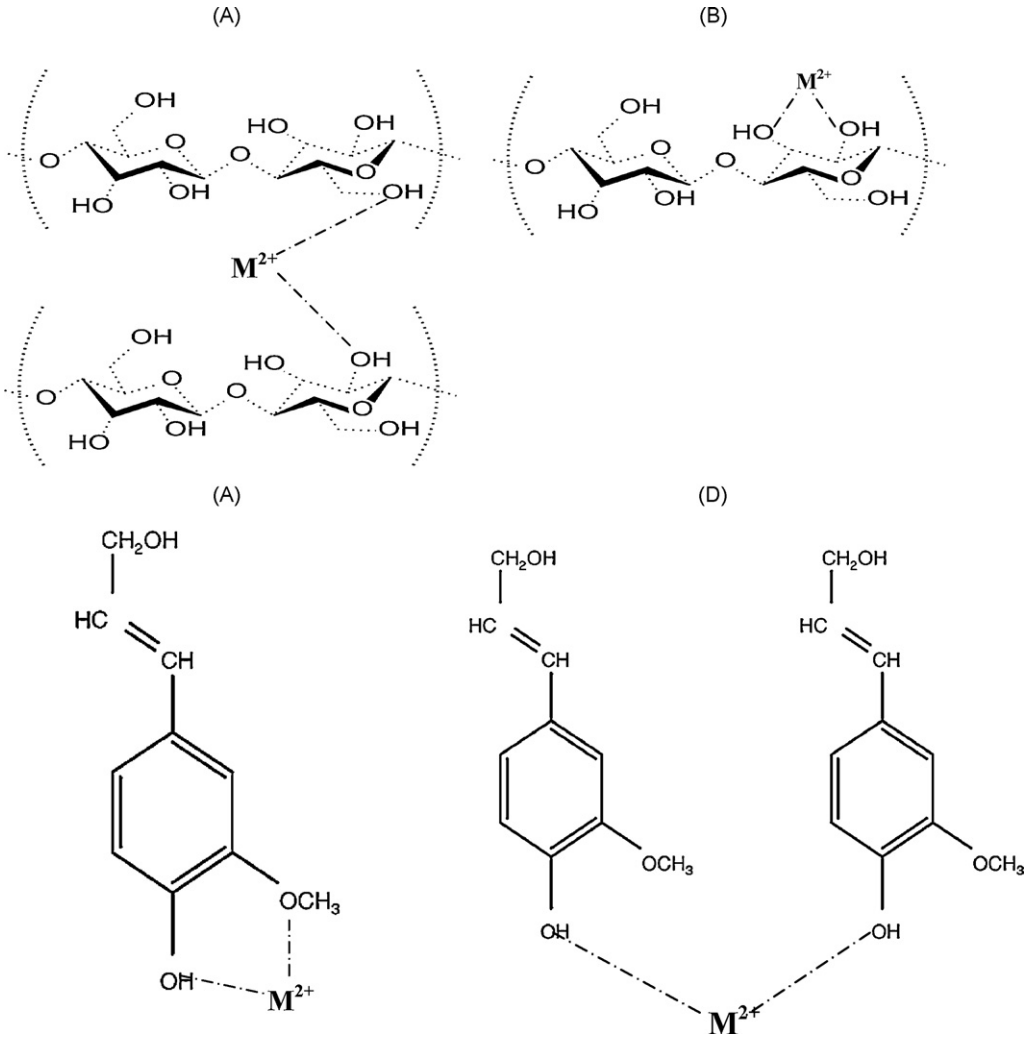

Fig. 6. Binding mechanism of the RDP, cellulose and lignin, respectively with Cu^{2+} and Cd^{2+}.

To investigate the dye orientation on the surface of the RDP, FTIR spectroscopy was used for MB, in powder form, and the RDP-MB loaded between 1800 and 1000 cm^{-1} (the figure is not shown here). For MB, the most important peaks are –C=C–,–C=N–, and–C–N–. The stretching bands related to these peaks are 1600 and 1342 cm^{-1}, respectively [21]. The peaks due to the –C=C–, –C=N–, and–C–N–stretching are weaker than the peaks for MB in its powder form. There are three possible orientations of MB adsorption on the RDP surface. These orientations are: (a) only one of the amino groups is mainly involved in the bonding to the RDP surface resulting in a localization of the charge, i.e. one resonance structure is frozen upon adsorption, (b) the aromatic rings of the dye orient perpendicularly to the RDP surface, and (c) the aromatic rings of the dye orient horizontally to the RDP surface. The possibilities of

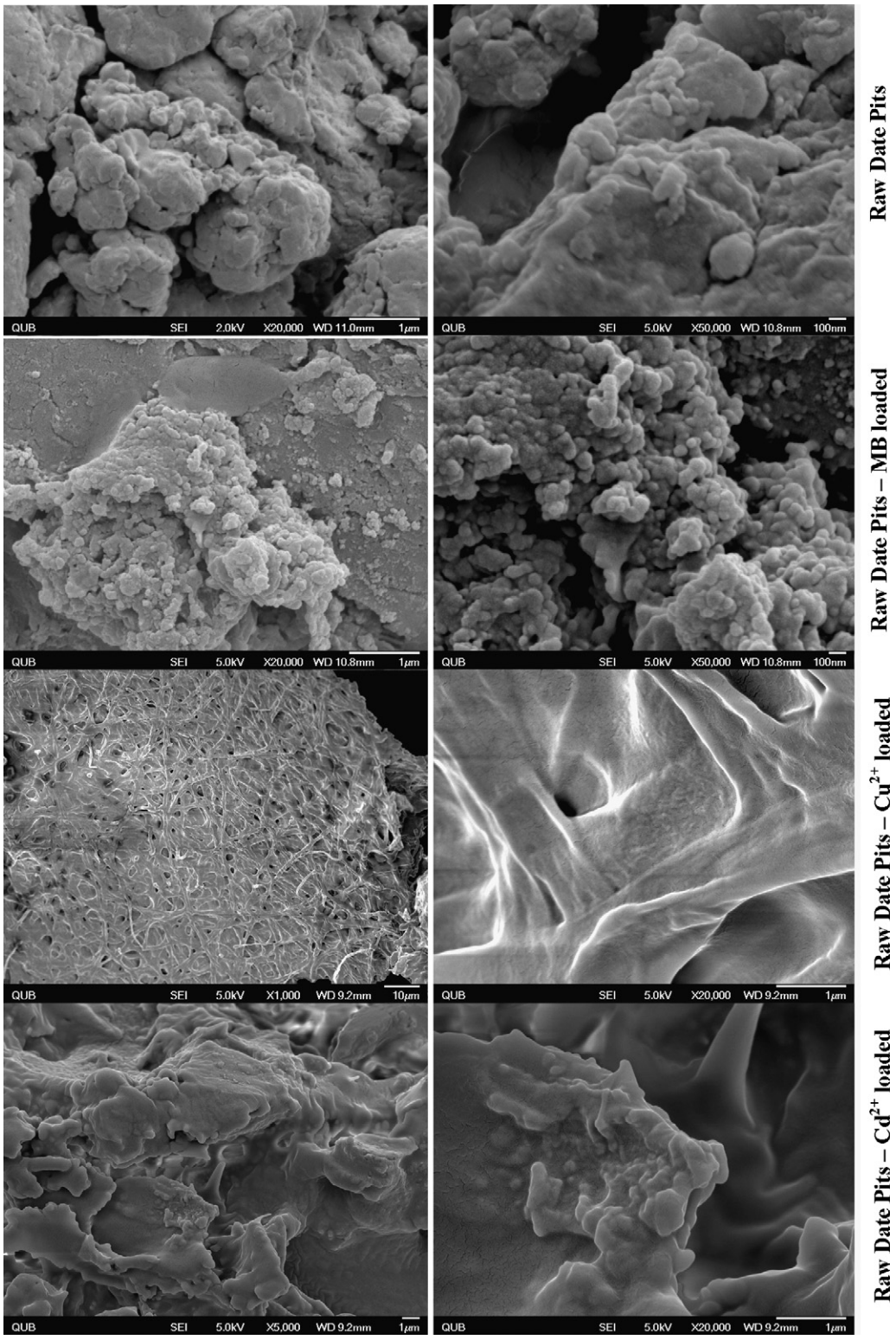

Fig. 7. SEM micrographs for the RDP, RDP-MB loaded, RDP-Cu^{2+} loaded and RDP-Cd^{2+} loaded samples, respectively.

MB orientation in the horizontal plane are preferable and achieved by forming a hydrogen bond between the hydrogen atoms of the silanol groups and the nitrogen atoms in MB or by electrostatic interaction induced by the resonance structure of MB. Imamura et al. [34] used infrared analysis to determine the orientations of the adsorbed MB and its congener on stainless steel surface. It was noted that the peaks due to –C=C– and –C=N– stretching, for the dyes adsorbed on the stainless steel plate, were strongly detected, while the–C–N–stretching was weaker than those for solution and powder samples. It was proposed that the transition moment of –C=C– and –C=N– stretchings are oriented perpendicular to the stainless steel surface and the transition moment of –C–N– stretching was less perpendicular. Such an orientation of the bonds could happen when the polyheterocycles of the dyes orient perpendicular to the stainless steel surface.

3.5.2. Proposed mechanisms for Cu^{2+} and Cd^{2+} adsorption

In relation with the results mentioned above, the present work shows that Cu^{2+} and Cd^{2+} is adsorbed by the RDP at about pH 4.0 as a result of three concurrent processes: complexation, adsorption, and hydrolysis-product precipitation. The –OH stretching vibration bands (3400 cm^{-1}) of the RDP are broadened and shift to a higher wavenumber after Cu^{2+} and Cd^{2+} adsorption. This indicates that stronger inter/intramolecular hydrogen bonds in the RDP have occurred after adsorption.

For metal ions, the stability of the complexes is determined largely by the basicity of the donor group, i.e. the availability of the electron, the greater the basicity the greater is the stability of the complex [35]. Copper is known to form complexes with very high stability despite a poor basicity of the donor group; fixation depends on the metal ion, on its chemistry, and its affinity to the ligand. Two types of fixation sites would coexist: the cellulose-OH sites involved in ion exchange and those taking part in adsorption and lignin-OH sites. Furthermore, fixation capacities are dependent on the metals adsorbed, it is higher for Cu^{2+} due to its strong affinity with hydroxyl functions onto the substrate and decreasing for Cd^{2+}. This probably means that the mechanisms A and D are predominant for Cu^{2+} adsorption (getting clear structure of cellulose fiber) and mechanisms B and C are predominant for Cd^{2+} adsorption (Fig. 6).

A model describing the process of Cu^{2+} and Cd^{2+} adsorption onto cellulose/lignin is proposed in Fig. 6.

3.6. Scanning electron microscope (SEM)

The RDP was examined in a scanning electron microscopy study. Fig. 7 shows the SEM micrographs of the RDP, RDP-MB loaded, RDP-Cu^{2+} loaded, and RDP-Cd^{2+} loaded samples. It shows evidence that the RDP structure was changed upon adsorbing the solutes studied. The SEM micrographs of the RDP-MB loaded samples exhibits a tendency to form spherical agglomerates while the RDP-Cu^{2+} loaded and RDP-Cd^{2+} loaded samples gives fibers/threads (clear structure of cellulose) and paste structure, respectively.

4. Conclusions

Knowledge of adsorption parameters is essential for understanding the adsorption mechanisms involved. The maximum adsorption capacities for MB, Cu^{2+}, and Cd^{2+} onto the RDP were reached after 72 h. The pH of the solute solution is a very important parameter since it affects the solute adsorption capacities on the RDP. For MB the adsorption capacities increased with the increase in pH. The opposite effect is observed for Cu^{2+} and Cd^{2+}. There is a slight effect of particle size of the RDP on adsorption of MB, Cu^{2+}, and Cd^{2+} at low initial solute concentrations but at higher concentrations an effect was observed. The results shows that the behavior of adsorption processes of Cu^{2+} and Cd^{2+} onto the RDP is almost linear and consequently, the Langmuir adsorption isotherm was not successfully applied. The experimental evidence indicates that an isotherm plateau was not reached. The isotherms exhibited the Freundlich behavior, which indicates a heterogeneous surface binding.

Surface functional groups on the RDP surface substantially influences the adsorption characteristics of MB, Cu^{2+}, and Cd^{2+} onto the RDP. The FTIR spectroscopy results of the samples showed clear differences both in the different absorbances and shapes of the bands and in their location. Two mechanisms were observed for MB adsorption onto the RDP, hydrogen bonding and electrostatic attraction, while other mechanisms were observed for Cu^{2+} and Cd^{2+}. For Cu^{2+}, binding two cellulose/lignin units together is the predominant mechanism. For Cd^{2+}, the predominant mechanism is by binding itself using two hydroxyl groups in the cellulose/lignin unit.

References

[1] Y.S. Al-Degs, M.I. El-Barghouthi, A.A. Issa, M.A. Khraisheh, G.M. Walker, Sorption of Zn(II), Pb(II), and Co(II) using natural sorbents: equilibrium and kinetic studies, Water Res. 40 (2006) 2645–2658.

[2] M.A. Al-Ghouti, M.A.M. Khraisheh, S.J. Allen, M.N. Ahmad, The removal of dyes from textile wastewater: a study of the physical characteristics and adsorption mechanisms of diatomaceous earth, J. Environ. Manage. 69 (2003) 229–238.

[3] D.L. Vullo, H.M. Ceretti, M.A. Daniel, S.A.M. Ramírez, A. Zalts, Cadmium, zinc and copper biosorption mediated by *Pseudomonas veronii* 2E, Bioresour. Technol. 99 (2008) 5574–5581.

[4] W. Zheng, X.-M. Li, Q. Yang, G.-M. Zeng, X.-X. Shen, Y. Zhang, J.-J. Liu, Adsorption of Cd(II) and Cu(II) from aqueous solution by carbonate hydroxylapatite derived from eggshell waste, J. Hazard. Mater. 147 (2007) 534–539.

[5] C.H. Weng, C.P. Huang, Treatment of metal industrial wastewater by fly ash and cement fixation, J. Environ. Eng. 120 (1994) 1470–1487.

[6] G. Crini, Non-conventional low-cost adsorbents for dye removal: a review, Bioresour. Technol. 97 (2006) 1061–1085.

[7] F. Banat, S. Al-Asheh, L. Al-Makhadmeh, Kinetics and equilibrium study of cadmium ion sorption onto date pits: an agricultural waste, Adsorpt. Sci. Technol. 21 (2003) 245–260.

[8] E.M. Saad, R.A. Mansour, A. El-Asmy, M.S. El-Shahawi, Sorption profile and chromatographic separation of uranium (VI) ions from aqueous solutions onto date pits solid sorbent, Talanta 76 (2008) 1041–1046.

[9] F. Banat, S. Al-Asheh, D. Al-Rousan, A comparative study of copper and zinc ion adsorption on to activated and non-activated date-pits, Adsorpt. Sci. Technol. 20 (2002) 319–335.

[10] F. Banat, S. Al-Asheh, L. Al-Makhadmeh, Utilization of raw and activated date pits for the removal of phenol from aqueous solutions, Chem. Eng. Technol. 27 (2004) 80–86.

[11] M.S. Rahman, S. Kasapis, N.S.Z. Al-Kharusi, I.M. Al-Marhubi, A.J. Khan, Composition characterisation and thermal transition of date pits powders, J. Food Technol. 80 (2007) 1–10.

[12] W.H. Barreveld, Date palm products. FAO agricultural services bulletin no. 101, Food and Agriculture Organization of the United Nations Rome, 1993.

[13] M.A. Khraisheh, M.A. Al-Ghouti, S.J. Allen, M.N. Ahmad, Effect of OH and Silanol groups in the removal of dyes from aqueous solution using diatomite, Water Res. 39 (2005) 922–932.

[14] D.W. O'Connell, C. Birkinshaw, T.F. O'Dwyer, Heavy metal adsorbents prepared from the modification of cellulose: a review, Bioresour. Technol. 99 (2008) 6709–6724.

[15] J.P. Chen, M. Lin, Equilibrium and kinetic of metal ion adsorption onto a commercial H-type granular activated carbon: experimental and modelling studies, Water Res. 35 (2001) 2385.

[16] E. Pehlivan, B.H. Yanık, G. Ahmetli, M. Pehlivan, Equilibrium isotherm studies for the uptake of cadmium and lead ions onto sugar beet pulp, Bioresour. Technol. 99 (2008) 3520–3527.

[17] V.M. Dronnet, C.M.G.C. Renard, M.A.V. Axelos, J.-F. Tbibault, Binding of divalent metal cations by sugar-beet pulp, Carbohydr. Polym. 34 (1997) 13–82.

[18] M. Streat, J.W. Patrick, M.J. Camporro Perez, Sorption of phenol and parachlorophenol from water using conventional and novel activated carbons, Water Res. 29 (1995) 467–472.

[19] L. Benefield, B. Weand, Process Chemistry for Water and Wastewater Treatment, Practice-Hall, U.S.A., 1982.

[20] W.J. Weber, P.M. McGinley, L.E. Katz, Review paper: sorption phenomena in subsurface systems: concepts, models and effects on contaminant fate and transport, Water Res. 25 (1991) 499–528.

[21] M.A.M. Khraisheh, M.A. Al-Ghouti, S.J. Allen, M.N.M. Ahmad, The effect of pH, temperature and molecular size on the removal of dyes from textile effluent using manganese oxides modified diatomite, Water Environ. Res. 79 (2004) 51–59.

[22] S.J. Allen, G. MaKay, K.Y.H. Khader, Equilibrium adsorption isotherms for basic dyes onto lignite, J. Chem. Technol. Biotechnol. 45 (1989) 291–302.

[23] M.M. Benjamin, J.O. Leckie, Multi-site adsorption of CD, Cu, Zn and Pb on amorphous iron oxyhydoxide, J. Colloid Interface Sci. 79 (1980) 209–221.
[24] S.J. Allen, G. McKay, K. Khader, Multi-component sorption isotherms of basic dyes onto peat, J. Environ. Pollut. 52 (1988) 39–53.
[25] K. Sing, The use of nitrogen adsorption for the characterisation of porous materials, Review, Colloids Surf. A Physicochem. Eng. Asp. 187–188 (2001) 3–9.
[26] W.C. Conner, J.F. Cevallos-Candau, E. Weist, J. Pajares, S. Mendioroz, A. Cortés, Characterization of pore structure: porosimetry and sorption, Langmuir 2 (1986) 151–154.
[27] Y.C. Chiang, P.C. Chiang, C.P. Huang, Effects of pore structure and temperature on VOC adsorption on activated carbon, Carbon 39 (2001) 523–534.
[28] O. Altin, H.Ö. Özbelge, T. Dogu, Effect of pH in an aqueous medium on the surface area, pore size distribution, density, and porosity of montmorillonite, J. Colloid Interface Sci. 217 (1999) 19–27.
[29] A.A. El-Hendawy, Variation in the FTIR spectra of a biomass under impregnation, carbonization and oxidation conditions, J. Anal. Appl. Pyrolysis 75 (2006) 159–166.
[30] K.K. Pandey, A.J. Pitman, FTIR studies of the changes in wood chemistry following decay by brown-rot and white-rot fungi, Int. Biodeterior. Biodegrad. 52 (2003) 151–160.
[31] C. Kaewprasit, E. Hequet, N. Abidi, J.P. Gourlot, Application of methylene blue adsorption to cotton fiber specific surface area measurement. Part I: methodology, J. Cott. Sci. 2 (1998) 164–173.
[32] R.S. Juang, F.C. Wu, R.L. Tseng, Mechanism of adsorption of dyes and phenols from water using activated carbons prepared from plum kernels, J. Colloid Interface Sci. 227 (2000) 437–444.
[33] A. Krysztafkiewicz, S. Binkowski, T. Jesionowski, Adsorption of dyes on a silica surface, Appl. Surf. Sci. 199 (2002) 31–39.
[34] K. Imamura, E. Ikeda, T. Nagayasu, T. Sakiyama, K. Nakanishi, Adsorption behaviour of methylene blue and its congeners on a stainless steel surface, J. Colloid Interface Sci. 245 (2002) 50–57.
[35] K.K. Krishnani, X. Meng, C. Christodoulatos, V.M. Boddu, Biosorption mechanism of nine different heavy metals onto biomatrix from rice husk, J. Hazard. Mater. 153 (2008) 1222–1234.